Pitfalls in evaluating permeability experiments with Caco-2/MDCK cell monolayers

Andrea Ebert [a,*], Carolin Dahley [a], Kai-Uwe Goss [a,b]

[a] *Department of Analytical Environmental Chemistry, Helmholtz Centre for Environmental Research (UFZ), Permoserstraße 15, Leipzig 04318, Federal Republic of Germany*
[b] *Institute of Chemistry, University of Halle-Wittenberg, Kurt-Mothes-Straße 2, Halle 06120, Federal Republic of Germany*

ARTICLE INFO

ABSTRACT

When studying the transport of molecules across biological membranes, intrinsic membrane permeability (P_0) is more informative than apparent permeability (P_{app}), because it eliminates external (setup-specific) factors, provides consistency across experiments and mechanistic insight. It is thus an important building block for modeling the total permeability in any given scenario. However, extracting P_0 is often difficult, if not impossible, when the membrane is not the dominant transport resistance. In this work, we set out to analyze P_{app} values measured with Caco-2/MDCK cell monolayers of 69 literature references. We checked the P_{app} values for a total of 318 different compounds for the extractability of P_0, considering possible limitations by aqueous boundary layers, paracellular transport, recovery issues, active transport, a possible proton flux limitation, and sink conditions. Overall, we were able to extract 77 reliable P_0 values, which corresponds to about one quarter of the total compounds analyzed, while about half were limited by the diffusion through the aqueous layers. Compared to an existing data set of P_0 values published by Avdeef, our approach resulted in a much higher exclusion of compounds. This is a consequence of stricter compound- and reference-specific exclusion criteria, but also because we considered possible concentration-shift effects due to different pH values in the aqueous layers, an effect only recently described in literature. We thus provide a consistent and reliable set of P_0, e.g. as a basis for future modeling.

1. Introduction

Transwell experiments with human colorectal adenocarcinoma (Caco-2) or Madin-Darby canine kidney (MDCK) cells are the gold standard for measuring *in vitro* permeabilities governing intestinal absorption of chemicals (Hubatsch et al., 2007). In these assays, the chemical crosses a cell monolayer grown on a permeable filter support, as well as the adjacent aqueous boundary layers (ABL; alternative: unstirred water layer, UWL). Two parallel permeation pathways across the cell monolayer need to be considered: (i) the paracellular pathway through tiny pores between the cells, and (ii) the transcellular pathway, where the chemical permeates the apical membrane, the cytosol, and the basolateral membrane (Bittermann and Goss, 2017). The paracellular pathway will dominate the passive permeation of strongly hydrophilic compounds such as ions, while the transcellular pathway will dominate for hydrophobic compounds (Artursson et al., 2012). The measured apparent permeability (P_{app}) for many hydrophobic compounds,

however, will not be determined by the actual membrane permeability, but will be limited by the diffusion through the ABL (Avdeef and Tam, 2010). P_{app} values measured *in vitro* can thus not be extrapolated 1 to 1 to *in vivo*, because both paracellular transport and the thickness of the ABL *in vitro* differ from *in vivo* (Avdeef et al., 2004). The same is true among experimental *in vitro* setups, and consequently the assays show high lab-to-lab variability (Lee et al., 2017). To extrapolate permeabilities *in vitro* to *in vivo*, or just to explain differences between different labs, it is necessary to introduce the intrinsic membrane permeability P_0. P_0 is defined here as the permeability of the neutral species across a single membrane barrier. In almost all cases, ionic permeability of ionizable compounds is insignificant (Ebert et al., 2018; Schwöbel et al., 2020), thus for the total membrane permeability (P_m) applies:

$$P_m = P_0 * f_n \tag{1}$$

where, f_n is the neutral fraction of the compound. Knowing the intrinsic permeability, total cell monolayer permeability can be reconstructed

---

from scratch. It allows modeling different scenarios, such as different ABL sizes and different experimental pH values.

There are many pitfalls in the determination of P_0. We discern between two major categories of problems that might lead to incorrect P_0: (i) An incorrect determination of P_{app}, thus making a correct extraction of P_0 impossible; (ii) A correct determination of P_{app}, but incorrect extraction of P_0.

There are many reasons that might lead to incorrect experimental P_{app} (Hubatsch et al., 2007), the major ones being leaky cell monolayers, measurements under non-sink conditions, and recovery issues (Heikkinen et al., 2009). These issues have been addressed in the past: cell monolayers are usually tested for leakiness (e.g. using Lucifer Yellow, mannitol or TEER) and leaky monolayers are discarded. Most experimenters comply with sink conditions, using smaller time steps and complete media exchange (Dahley et al., 2023; Neuhoff et al., 2003), or simply recalculate P_{app} for non-sink conditions (Von Richter et al., 2009; Wohnsland and Faller, 2001). Note that these corrections are not valid if a pH difference is applied across the monolayer, then a more sophisticated equation needs to be used for acids and bases (Avdeef, 2012). At the end of the experiment, usually a mass balance is done to check for recovery issues. Especially extremely hydrophobic compounds show a poor mass balance. The compound may adsorb to the experimental setup, or is retained within the cell, e.g. bound to lipid or proteins, or may be metabolized.

According to Neuhoff (2005), P_{app} can be corrected for recovery as follows:

$$P_{app,corrected} = \frac{P_{app} * 100}{Recovery} \tag{2}$$

But even with correctly determined P_{app}, an extraction of incorrect P_0 is likely. Between a minimal P_{app} dominated by paracellular transport, and a maximum P_{app} dominated by the ABL, only a small permeability-window remains where P_{app} is dominated by P_m, allowing the extraction of P_0, see Fig. 1. Outside this range, it is not possible to extract P_0, only a maximum or minimum value.

However, it is not always easy to assess which sub-process dominates a measured P_{app} value. Paracellular transport is not only compound specific, but also depends on the cell line and the experimental setup (Avdeef, 2010). The size of the ABL is setup specific, and depends on the applied shaking or stirring speed (Adson et al., 1995; Karlsson and Artursson, 1991; Korjamo et al., 2008). For ionizable compounds, it is sometimes possible to target the P_m-dominated range by adapting the experimental pH: one uses the fact that permeation through the ABL remains the same with decreasing neutral fraction, but permeation through the membrane decreases (assuming that only the neutral fraction is permeable). This way, the resistance of the membrane can be increased relative to the ABL, and, ideally, membrane permeation dominate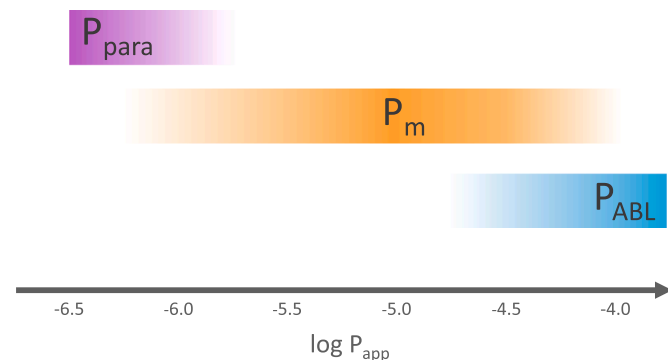s, which then allows an extraction of the P_0 value. In this regard, a well-known method is the pK_a-flux method, which, however, may lead to errors if a pH difference is applied across the cell monolayer, due to resulting concentration-shift effects in the aqueous layers (Dahley et al., 2023). These concentration-shift effects may increase (or decrease) the resistance of the aqueous layers, and if not considered, can lead to a severe underestimation of P_0 for hydrophobic compounds (Dahley et al., 2023). These recent findings make a re-evaluation of the published literature desirable in terms of P_0 values extracted from P_{app}, since ABL-limitations might have been overlooked.

Also active transport may lead to incorrect P_0 if overlooked: if $P_{app}^{a \to b}$ is affected by active efflux in the apical membrane, the extracted P_0 will be underestimated; in case of active influx, P_0 will be overestimated. In principle, a method (Avdeef, 2012) exists to calculate out the effect of active transport by taking the mean of the P_{app} values in both directions (apical to basolateral and vice versa), but it is only valid in very specific circumstances, as we will show below. Ideally, to extract P_0, an inhibitor is used in the experiment and the transport is checked in both directions (apical to basolateral and vice versa) or active transport is saturated by increased compound concentrations. But such high concentrations used to avoid active transport pose another potential problem: a limitation by proton transport might lead to pH gradients within the ABL adjacent to the monolayer, a problem which has been extensively discussed in biophysics with black lipid membranes (Antonenko et al., 1993; Pohl et al., 1997) but which has to our knowledge not been checked for transport experiments with cellular monolayers so far.

An additional problem when extracting P_0 is the handling of zwitterions: For zwitterions, it is usually assumed that only the permeability of all net zero charge compounds is measured (Tam et al., 2010). Our hypothesis is that only the neutral fraction, not the zwitterionic fraction can permeate the membrane. This is not a new idea, it has already been stated in Bermejo et al. (2004) that for fluoroquinolones the neutral species dominates membrane permeability. Still, in most cases literature data are evaluated as if the net zero charge species is identical to the neutral species, even in the classical textbook of Avdeef (2012). Zwitterions will thus be considered in a separate publication, as they would go beyond the scope of this work, and are excluded here from re-evaluation.

In this work, we will take a closer look at a multitude of published Caco-2 and MDCK P_{app} values, and try to extract reliable intrinsic permeability values. To exclude ABL effects and influence of paracellular transport, we will determine individual ABL sizes and factors for paracellular transport of the respective references. The possible influence of measurements under non-sink conditions, low recovery, or potential pH gradients within the ABL are discussed as well. In the end, we will revise and extend the list of neutral P_0 values published in the classical textbook of Avdeef (2012, Table 8.6).

2. Methods

2.1. Theory

For the permeation across a cell monolayer, we consider several resistances in series: the aqueous boundary layer on the apical side, the resistance of the cell monolayer, the resistance of the filter, and the resistance of the aqueous boundary layer on the basolateral side. The permeation through the cell monolayer consists of two parallel diffusion paths, the transcellular pathway (two membranes and the cytosol) and the paracellular pathway. To extract the intrinsic neutral membrane permeability P_0 from measured apparent permeabilities, the following equation describing the apparent permeability P_{app} in apical to basolateral direction was used (Dahley et al., 2023):

$$P_{app}^{a \to b} = \frac{1}{\frac{1}{P_{ABL,a}} + \frac{1}{\left(P_{trans}^{a \to b} + P_{para}\right)} + \frac{1}{S_{ABL,b}^{a \to b}} * \left(\frac{1}{P_{filter}} + \frac{1}{P_{ABL,b}}\right)} \tag{3}$$

Fig. 1. Depiction of the small range of P_{app} (unit cm/s) dominated by P_m that allows for the extraction of P_0 in typical permeability studies with Caco-2 or MDCK cell monolayers.

where, $P_{ABL,b}$ and $P_{ABL,a}$ are the permeability through the unstirred water layer adjacent to the cell monolayer on the basolateral and apical side respectively, P_{filter} is the permeability through the filter, P_{trans} is the transcellular permeability, and P_{para} is the paracellular permeability. Details on the calculation of the single parameters can be found in Dahley et al. (2023).

The concentration-shift factor $S_{ABL,b}^{a \rightarrow b}$ arises for ionizable compounds if a pH difference is applied across the cell monolayer and is described by:

$$S_{ABL,b}^{a \rightarrow b} = \frac{\left(P_{trans}^{a \rightarrow b} + P_{para} \right)}{\left(P_{trans}^{b \rightarrow a} + P_{para} \right)} \tag{4}$$

With the transcellular permeabilities being:

$$P_{trans}^{a \rightarrow b} = \frac{1}{\frac{1}{f_{n,a} * P_0 * 24} + \frac{1}{\frac{f_{n,a}}{f_{n,cyt}} * P_{cyt}} + \frac{1}{f_{n,a} * P_0}} \tag{5}$$

$$P_{trans}^{b \rightarrow a} = \frac{f_{n,b}}{f_{n,a}} * P_{trans}^{a \rightarrow b} \tag{6}$$

where, $f_{n,a}$, $f_{n,b}$ and $f_{n,cyt}$ are the respective neutral fractions in the apical and basolateral compartment and in the cytosol. P_{cyt} is the permeability through the cytosol, P_0 is the intrinsic neutral membrane permeability. The factor 24 accounts for the increased permeation area due to microvilli on the apical side (Palay and Karlin, 1959). This factor of 24 is subject to uncertainties, lower values have been reported for MDCK cells (Butor and Davoust, 1992). Also, the microvilli in Caco-2 cells and MDCK cells exhibit differences in their packing density and spatial arrangement (Meng et al., 2017). For simplicity, we use the factor of 24 in our evaluation for both cell types. This might underestimate the resistance of the apical membrane, and thus extracted P_0 might be underestimated by less than a factor of 2.

$S_{ABL,b}^{a \rightarrow b}$ is best explained by its extremes: (i) it will simply be 1 in absence of a pH difference, and if P_{para} dominates permeation, because both charged and neutral species permeate by the paracellular pathway and diffuse through the ABL. (ii) If the transcellular permeation dominates, the factor will be $\frac{f_{n,a}}{f_{n,b}}$. This is a consequence of only the neutral species permeating the cell membrane, while both charged and neutral species permeate the ABL. When the concentration gradient across the membrane is determined by the neutral species only, the neutral concentration adjacent to the membrane on the basolateral side directly depends on the neutral concentration on the apical side. For very high membrane permeabilities (as compared to ABL permeabilities), the neutral concentrations adjacent to the monolayer are almost identical. Yet, the total concentrations differ due to the difference in ionic fractionation as a consequence of the pH difference. The concentration gradient across the ABL is thus changed accordingly.

Often, both the paracellular and transcellular route contribute to the concentration-shift effect, and $S_{ABL,b}^{a \rightarrow b}$ needs to be calculated according to Eq. (4). The concentration-shift can either be positive, increasing the total compound concentration, or negative, decreasing the total compound concentration.

2.2. Calculation of fractions

To extract a compound's intrinsic neutral permeability, the neutral fractions at the experimental pH need to be known. For monoprotic acids and bases, Henderson-Hasselbalch was used to determine the fraction of the neutral and ionic species from the pK_a. For multiprotic compounds, the fractions were calculated as described in Escher et al. (2020). If available, experimental pK_a values were preferred, otherwise values were predicted using ACD/pK_a GALAS from ACD percepta (2020 release) and JChem for Excel (JChem for Office 20.2.0.589, 2020). All compounds where the strongest basic pK_a exceeded the strongest acidic

pK_a were categorized as zwitterions and not further evaluated here. Permanently charged compounds for which no neutral species exists were also not included in the evaluation. The experimental pK_a values from literature and predicted pK_a values used can be found in Table S2-1 in Supporting Material 2.

To calculate the fractions within the cell cytosol, the pH in the cytosol (pH_{cyt}) was approximated from the pH in the apical compartment (pH_a) as described in Dahley et al. (2023):

$$pH_{cyt} = 0.7027 * pH_a + 2.4854 \tag{7}$$

2.3. Extraction of P_{app} from literature

Ideally, P_{app} values from literature were directly read from tables, or if not stated, read from graphs using the software Webplotdigitizer (Rohatgi, 2022). We decided against using mean values of P_{app} from different references for evaluation, because some P_{app} values for a specific compound might be limited by the ABL, paracellular transport or active transport in one setup, but limited by membrane permeability in another setup (different pH, smaller ABL size, inhibitor, tighter junctions). Values measured with inhibitor were always preferred if several values were stated. If flux was measured in both directions, P_{app} in a to b direction was used for the extraction of P_0, but only if the efflux ratio was below 1.5. If only data showing active efflux was available to evaluate a compound, the P_{app} in b to a direction was considered as well, but only in so far as to provide a maximum value to compare with the dataset of Avdeef (2012). We evaluated data from 59 different references (Agarwal et al. (2007), Alsenz and Haenel (2003), Artursson and Karlsson (1991), Aungst et al. (2000), Bednarczyk (2021), Bermejo et al. (2004), Bhardwaj et al. (2005), Bokulic et al. (2022), Braun et al. (2000), Camenisch et al. (1998), Crowe (2002), Dahley et al. (2023), De Souza et al. (2009), Desmeules et al. (2008), Furubayashi et al. (2020), Gan et al. (1998), Garberg et al. (2005), Hayeshi et al. (2006), Irvine et al. (1999), Karlsson et al. (1999), Karlsson and Artursson (1991), Katragadda et al. (2008), Korjamo et al. (2008), Lee et al. (2005), Lentz et al. (2000a, 2000b), Liang et al. (2000), Mahar Doan et al. (2002), Maier-Salamon et al. (2006), Nagahara et al. (2004), Neuhoff et al. (2007, 2005, 2003), Obradovic et al. (2007), Pade and Stavchansky (1997), Polli et al. (2001), Potter et al. (2015), Psimadas et al. (2012), Raeissi et al. (2010), Robertson et al. (2005), Rodríguez-Ibáñez et al. (2006), Ruiz-García et al. (2002), Schrickx and Fink-Gremmels (2007), Skolnik et al. (2010), Sohlenius-Sternbeck and Terelius (2022), Soldner et al. (2000), Summerfield et al. (2007), Thiel-Demby et al. (2009), Troutman and Thakker (2003), Volpe (2004), Von Richter et al. (2009), Wang et al. (2005), Yamashita et al. (2000), Yazdanian et al. (1998), Yee (1997), Young et al. (2006), Yu and Zeng (2010), Zhang et al. (2022) and Zhao et al. (2009)). The selection is by no means exhaustive. If a compound was stated in several references, the crucial reference for evaluation of P_0 is listed in Table S2-2.

2.4. Aqueous boundary layers

To extract intrinsic permeabilities from apparent permeabilities, the influence of the ABL has to be excluded, otherwise P_0 might be underestimated by several orders of magnitude. We used compounds with very high intrinsic permeabilities as markers for ABL permeability, such as testosterone, antipyrine and caffeine (for a full list see Table S1-1 in Section S1-1 in the Supporting Material 1). Neutral markers could reliably be used to extract the total size of the ABL. Yet, if pH differences between the compartments are present, the permeation through the ABL in the acceptor compartment becomes pH-dependent, so the determination of the individual ABL sizes was necessary. Ionic compounds of high permeability such as propranolol, metoprolol or naproxen were used to determine the thickness of apical and basolateral ABL individually.

Typical markers for membrane permeability were not available for

all references. If reported P_{app} were only in the paracellular range, knowledge of the ABL was not possible, but also not necessary for the evaluation. If a reference with similar experimental setup was available, e.g. 12 well, 450 rpm, and the compounds of highest P_{app} were well matched with the reference's P_{app}, the ABLs of both references were assumed equal for our evaluation.

If there was no experimental uncertainty, any P_{app} slightly lower than the respective limiting P_{ABL} could in theory be used to calculate P_0 considering the influence of the aqueous layers (apical ABL, cytosol, filter, basolateral ABL). In reality, there is a significant variance between measurements considered as identical and also uncertainties in the determined ABL sizes, which makes it difficult to distinguish between a P_{app} which is slightly or completely limited by aqueous layers. We thus introduce $P_{infinite}$, which refers to the expected permeability if P_0 is assumed infinite, and thus represents the resistance posed by the aqueous layers alone (ABL, cytosol, filter). Here, any P_{app} less than a factor of 2 below $P_{infinite}$ was deemed to be limited by the ABL. In that case, no P_0 could be extracted, and only a lower limit of P_0 could be determined. $P_{infinite}$ was calculated according to Eq. (S1-1) (Section S1-2) using the extracted ABL size of the respective reference.

2.5. Paracellular transport

To extract intrinsic permeabilities from apparent permeabilities, the influence of paracellular transport has to be excluded, otherwise P_0 might be overestimated by several orders of magnitude. We used compounds with very low permeabilities as markers for paracellular transport, such as acyclovir, mannitol and sumatriptan (for a full list see Table S1-2 in Section S1-3). Typical markers for paracellular transport were not available for all references. If all P_{app} values reported in a reference were only in the high permeability range, it was not possible to obtain knowledge of the paracellular transport, but also not necessary for the evaluation.

To assess the influence of paracellular transport, compound specific paracellular transport was calculated with the corrected Avdeef method for a typical cell assay as described in Bittermann and Goss (2017). Experimental P_{para} of marker compounds were compared to the calculated values, and the mean of the quotient from experimental and calculated values was included in the calculation of P_{para} as a reference specific factor. All calculated P_{para} were multiplied with this reference specific factor to approximate a reference specific P_{para}. These P_{para} were then used to assess whether a P_{app} is limited by paracellular transport, or used for the calculation of P_0 from P_{app}. Here, P_{app} less than a factor of 2 above the predicted P_{para} was deemed limited by paracellular transport. If no reference specific P_{para} could be determined, a factor of 1 was used for the calculations.

Although P_{para} can be predicted and possibly adapted to individual laboratories, these predictions are not as reliable as measurements over several pH values. But one has to keep in mind that differences in paracellular transport between the charged and uncharged species alone can lead to pH-dependencies (Avdeef, 2010).

2.6. Extraction of P_0

Eq. (3) was used to extract P_0 from P_{app} values, considering the determined setup specific ABL sizes, and the calculated compound and setup specific P_{para}. In case of more than two pH-dependent P_{app} values from one reference for one compound, the fit was done in Igor Pro 7 (WaveMetrics Inc., Lake Oswego, USA), in case of less data points, for simplicity the Excel Solver add-in program was used to extract P_0. To generate lower limits that consider a possible false estimation of the ABL size, P_0 values were calculated in the case of an insubstantial contribution of P_{ABL} using Eq. (S1-2). To generate upper limits that consider a possible false estimation of P_{para}, P_0 values were calculated in case of an insubstantial contribution of P_{para} using Eq. (S1-3). If possible, all three values (P_0, upper limit, lower limit) were determined for each

compound, and are stated in Table S2-2. ABL size could not be considered in the calculations when P_{app} exceeded $P_{infinite}$, in that case it was only possible to generate lower limits for P_0. P_{para} could not be considered in the calculations when the calculated P_{para} exceeded P_{app}, in that case it was only possible to generate upper limits for P_0.

2.7. Recovery: 3-compartment model

To check the P_{app} of likely ABL-limited compounds for recovery issues, we here propose the use of a 3 compartment model for reversible first-order kinetics (Larisch and Goss, 2017), see Fig. 2.

Back- and forward-diffusion between three different compartments (apical, cell monolayer, basolateral) of different volumes is described by the rate constants k. For ABL-limited compounds, the rate constants represent the diffusion across the ABL and the respective membrane. To account for the increased sorption capacity of the cell monolayer, the volume of the cell monolayer is adapted to also represent sorption to lipids and proteins, see more details in Section S1-4 and Table S1-3. The output of the model are the concentrations within the single compartments over time. From the mass balance at the end of the simulated time, recovery can be determined. In principle, the model can also be used to check if sink conditions are fulfilled.

2.8. Proton flux limitation

Both the neutral and charged fraction can permeate the ABL, which makes pH-dependent measurements advantageous. With decreased neutral fraction, the resistance for membrane permeation increases, yet ideally the resistance for the diffusion through the ABL remains constant. This assumes that there is no proton flux limitation: When a compound crosses the ABL in its charged form, it either has to pick up a proton (acid) or discard a proton (base) to be able to cross the membrane in its neutral state. These protons need to cross the ABL, either freely dissolved or carried by buffer molecules. If this process becomes limiting, for example in poorly buffered systems or at high compound concentration, pH gradients will develop within the ABL, which may ultimately affect membrane permeation. To estimate this effect, we used the model of Antonenko et al. (1993, 1997). For specific buffer and compound concentrations, specific pH values, ABL-size and the compound's membrane permeability, the model will give the pH and compound gradients across the ABL, as well as the resulting P_{app}. The model has been validated for measurements in BLM, but has so far not been used in Caco-2/MDCK assays.

To adapt the model to our application, the equations were adapted to reflect asymmetric ABLs as is usual in Caco-2/MDCK assays (Dahley et al., 2023; Korjamo et al., 2008). Also, a higher number of buffers was introduced into the model, to account for typical incubation media such as Hank's balanced salt solution (HBSS), see Table S1-4. Detailed changes to the equations can be found in Section S1-5.

The model was created to simulate the pH across one single membrane. Since the apical membrane is assumed to have a larger surface area than the basolateral membrane by a factor of about 24 (Palay and Karlin, 1959), the cell monolayer is still well approximated by a single membrane if cytosolic resistance can be neglected. Paracellular effects play no role, because proton flux limitations only affect hydrophobic
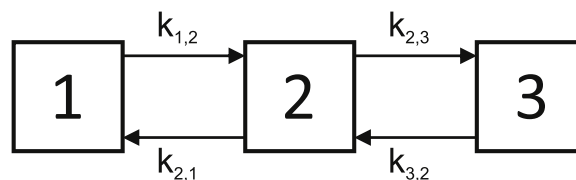
Fig. 2. Three-compartment system with first-order back-and-forth kinetics. 1, apical compartment; 2, cell monolayer; 3, basolateral compartment. With diffusive rate constants k.

compounds that are ABL-limited.

2.9. Correction for non-sink conditions

Mathematical corrections for P_{app} measured under non-sink conditions can already be found in literature (Tran et al., 2004; Wohnsland and Faller, 2001), but most equations do not consider possible pH differences across the cell monolayer, even though these are quite common. If the neutral fraction in the basolateral compartment exceeds the neutral fraction in the apical compartment, the apparent permeability in b to a direction will be higher than in a to b direction (without even considering possible active transport)(Neuhoff et al., 2005), and thus a relevant backflow will be reached at lower concentrations in the basolateral compartment. Considering the pH difference between donor and acceptor compartment, the apparent permeability can be corrected *via*

$$P_{app} = -\frac{\frac{V_D * V_R}{A * t}}{\left(V_D * \frac{f_{n,R}}{f_{n,D}} + V_R\right)} * \ln\left(1 - c_R * \left(\frac{V_D * \frac{f_{n,R}}{f_{n,D}} + V_R}{c_{D,0} * V_D}\right)\right) \tag{8}$$

where, V_D and V_R are the volume of the donor and acceptor compartment respectively, c_R is the concentration in the acceptor compartment after incubation time t, A is the filter area, $c_{D,0}$ is the initial donor concentration, and $f_{n,R}$ and $f_{n,D}$ are the compound's neutral fraction in
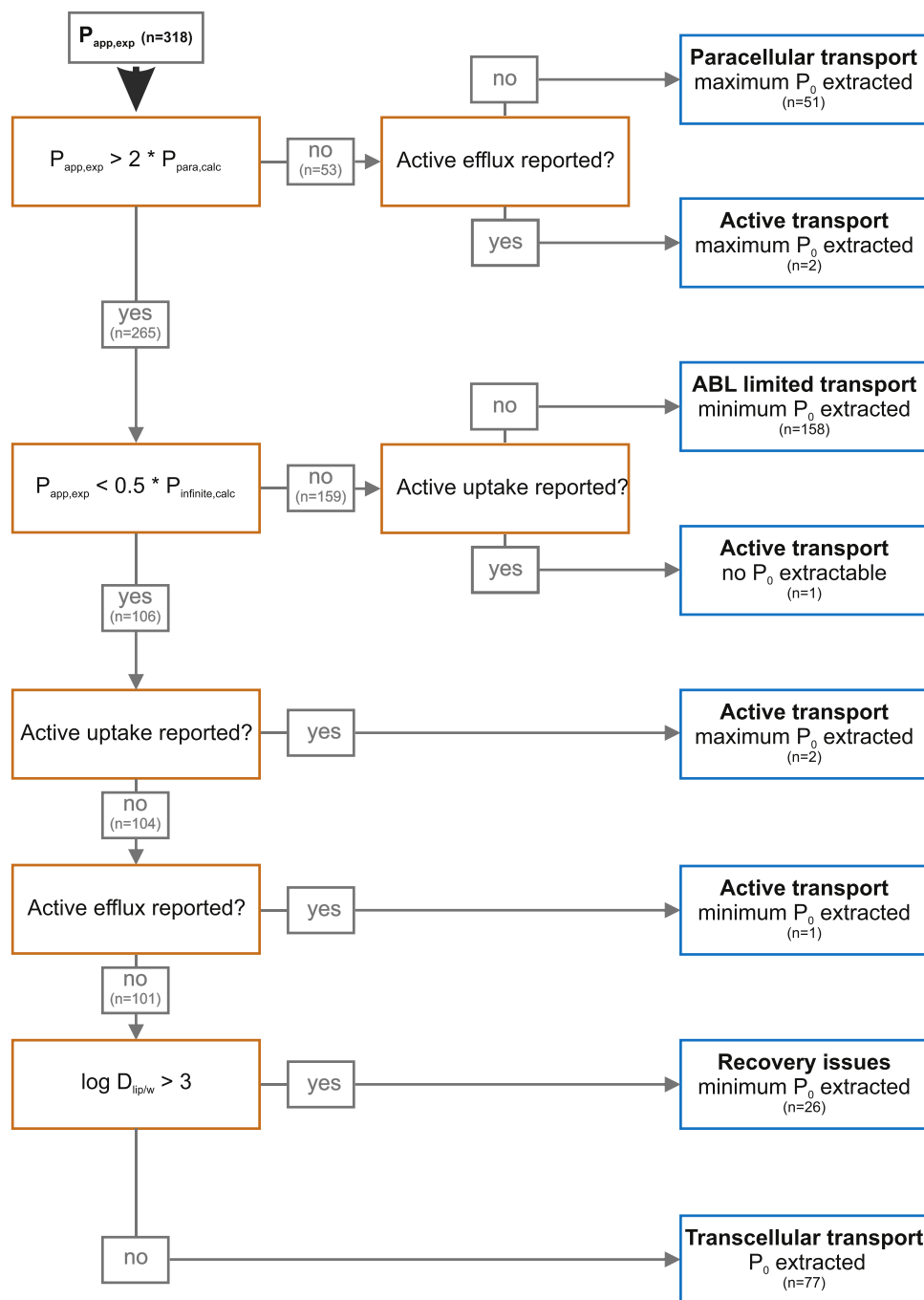

Fig. 3. Decision tree for the extraction of P_0 from published P_{app}. Six compounds were added in the category recovery issues although they did not fulfill the log $D_{lip/w}$>3 criterium, see section recovery for more details.

the acceptor and donor compartment respectively.

Eq. (8) is derived from the differential equation:

$$\frac{dc_R}{dt} = \frac{P_{app} * A}{V_R} * \left(c_D * f_{n,D} - c_R * f_{n,R}\right) \tag{9}$$

It assumes that only the neutral species can permeate the cell monolayer. Note that the correction from Eq. (8) is only valid in the range of high transcellular permeability. If paracellular transport dominates, both the neutral and charged species can permeate the cell monolayer, nullifying our assumption for the differential Eq. (9).

Active transport might also lead to relevant backflow, but is not considered here. For a more sophisticated sink correction under applied pH differences, see Eq. (A7.28a) in Avdeef (2012).

3. Results and discussion

3.1. Extracted P_0

In total, we collected P_{app} values measured in Caco-2 or MDCK cells for 395 different compounds, from 59 references. Of these compounds, 5 permanent ions and 72 zwitterions were not considered in this work, because zwitterions will require a different evaluation approach. The remaining 318 compounds were analyzed according the decision tree depicted in Fig. 3 (For more details, see the methods section). Intrinsic membrane permeabilities for 77 compounds could be extracted, the resulting P_0 are listed in Table 1. For 55 compounds, only an upper limit of P_0 could be extracted, since P_{app} could not be discerned from paracellular transport (51 compounds), or the compounds showed active transport (4 compounds). For 185 compounds, only a lower limit could be extracted for P_0, since transport was either not distinguishable from ABL-limited transport (158 compounds), dominated by active efflux (1 compound), or dominated by recovery issues (26 compounds). For one compound, d-phenylalanyl-l-proline, no P_0 limit could be extracted, because active uptake resulted in an ABL-limited P_{app}, and a distinction between upper and lower limit was thus not possible. A list of all P_0 limits can be found in the Tables S1-5 and S1-6 in Section S1-6. See Tables S2-1, S2-2 and S2-3 for a more detailed list containing chemical properties and all extracted P_0 values.

3.2. Reliability of extracted P_0

Note that due to uncertainties in the estimation of P_{ABL} and P_{para}, and the determination of P_{app}, only the P_{app} values not exceeding half of $P_{infinite}$ and exceeding P_{para} by more than a factor of 2 were considered for the extraction of P_0. This conservative approach, which may fail to detect some membrane permeabilities that could after all be extracted, was implemented to extract a consistent and reliable data set of P_0. In order to further categorize the reliability, extracted P_0 were either marked as category 1 if there were no obvious problems in the evaluation, or category 2 if evaluation was problematic. Possible reasons for problematic evaluation were: known active transport in absence of inhibitor (e.g. bosentan); inexplicable contradictions between different references (e.g. digoxin, see Fig. S1-1a in Section S1-7), or even within different measurements in one reference; inexplicable pH-dependence (e.g. terazosin, see Fig. S1-1b); uncertain pK_a (e.g. guanoxan); substantial metabolism (e.g. zidovudine). For apparent permeabilities measured without the use of inhibitor or without the measurement of both "apical to basolateral" and "basolateral to apical" direction, the risk of underestimating (in case of active efflux) or overestimating (in case of active uptake) P_0 is increased. Thus, for the reliability categorization, the category (1 or 2) is followed by the additional descriptors "a" for when inhibitor was used, no efflux ratio was measured or both, or "b" in the absence of any inhibitor. Small uncertainties in P_0 will always remain, since differences due to different cell lines may be possible (Lea, 2015). When comparing very reliable P_{app} values from different references, we still observed an unexplained difference of up to a factor of about 5, for

Table 1

Extracted intrinsic membrane permeabilities P_0: Compound name, extracted intrinsic membrane permeability P_0, and categorized reliability of the extracted P_0, P_0 extracted by Avdeef[a].

Compound name	log P_0 in cm/s Re-evaluated	Reliability[b]	log P_0 in cm/s Avdeef
acebutolol	−4.15	1a	−4.19
acetaminophen	−4.35	1b	−4.34
acetylsalicylic acid	−1.35	1b	−1.53
alfuzosin	−4.22	1a	−4.27
amantadine	−0.82	1a	−2.17[c]
amrinone	−4.85	1b	n.d.
atenolol	−4.38	1b	−4.34
atropine	−1.85	1b	n.d.
azithromycin	−2.72	2a	n.d.
belinostat	−5.17	1b	n.d.
benzylpenicillin	−2.95	1b	n.d.
bosentan	−4.53	2b	n.d.
bremazocine	−2.40	1a	−2.86
chloramphenicol	−4.14	1a	−4.47
chloroquine	0.05	1a	−1.18c
cimetidine	−6.13	1a	−6.06
creatinine	−6.27	1a	−5.9
cyclosporin	−5.18	1a	−5.24
cymarin	−5.55	1b	n.d.
dexamethasone	−4.14	2b	−4.65
diclofenac	0.54	1a	−1.07c
digoxin	−4.87	2a	−5.43
dipyridamole	−4.56	1a	−3.86
disopyramide	−2.07	1b	n.d.
dopamine	−3.13	1b	n.d.
ephedrine	−2.85	1a	−2.91
etoposide	−6.66	1a	−6.11
famciclovir	−4.78	1a	−4.79
fluconazole	−4.28	1a	n.d.
fluvastatin	−1.88	1a	−1.33
fosinopril	−2.87	1b	n.d.
furosemide	−2.32	2b	−3.5[c]
glibenclamide	−2.37	1a	n.d.
glipizide	−2.26	2b	−2.47
guanfacine	−4.72	1a	−4.73
guanoxan	0.31	2b	n.d.
hydrochlorothiazide	−6.48	1b	−6.32
hydrocortisone	−4.37	1b	−4.63
ketoprofen	−0.90	2b	−1.23
meprobamate	−4.31	1a	−4.94
methylprednisolone	−4.46	1b	−4.63
metolazone	−5.43	2b	n.d.
metoprolol	−1.40	1a	−1.85
minoxidil	−5.82	1a	−5.68
morphine	−4.33	1a	−4.55
nadolol	−5.16	1b	−4.47
nalbuphine	−3.28	1a	−3.3
naproxen	−0.45	1a	−0.95
pemirolast	−2.86	1a	n.d.
pindolol	−1.83	1a	−2.22
prednisolone	−4.98	1b	n.d.
propylthiouracil	−4.14	1b	−3.76
quinidine	−2.02	1a	−3.31c
ranitidine	−5.51	1a	−5.27
rizatriptan	−3.69	1a	−4.18
Salicylic acid	−0.20	1a	−0.43
scopolamine	−3.22	1a	−4.57c
semagacestat	−5.38	1b	n.d.
sotrastaurin	−4.18	1b	n.d.
sulfadiazine	−3.97	1a	n.d.
sulindac	−1.98	1b	n.d.
talinolol	−4.05	1a	n.d.
terazosin	−4.71	2b	n.d.
theophylline	−3.96	1a	−4.17
tiacrilast	−2.01	2b	n.d.
tolbutamide	−1.84	1a	n.d.
triamterene	−4.59	1a	n.d.
trimethoprim	−3.92	1b	−3.95
uracil	−5.31	1b	n.d.
urapidil	−4.24	1b	n.d.
urea	−5.40	1a	n.d.

(continued on next page)

Table 1 (*continued*)

Compound name	log P_0 in cm/s Re-evaluated	Reliability[b]	log P_0 in cm/s Avdeef
valproic acid	−2.15	2b	n.d.
venlafaxine	−0.82	1a	−2.84c
vinblastine	−4.27	1a	−4.5
zidovudine (AZT)	−3.94	2a	−4.97c
zolmitriptan	−3.85	2a	−4.26
zomepirac	−1.18	1b	−1.51

[1] Table 8.6 in Avdeef (2012).
[b] As described in the section "Reliability of extracted P_0".
[c] Differs by more than one log unit from our re-evaluated value that was based on new experimental data.

example in the case of salicylic acid.

3.3. Comparison to P_0 from literature

The list of 195 P_0 values (143 non-zwitterionic compounds) extracted by Avdeef (2012) is to our knowledge the most extensive list of intrinsic membrane permeability published so far. All 143 non-zwitterionic compounds were part of our extended dataset of 318 compounds. Yet, despite our extended dataset we extracted a much lower number, namely 77 P_0 values. Of these, 29 were not included in the original list of Avdeef. Thus, we excluded 95 compounds for which no reliable extraction was possible according to our criteria. This may be surprising, considering that Avdeef had spent a lot of effort in curating apparent permeability data from ABL effects and effects of paracellular transport.

The following differences apply:

- More recent datasets are included in the evaluation, especially such as Dahley et al. (2023) that focused on very hydrophobic compounds and used the iso-pH method (no pH difference) to avoid negative concentration-shift effects.
- Recently, we detected that pH differences between the aqueous layers (ABL, cytosol, filter) can lead to concentration-shift effects that have not been considered in the evaluation of P_0 before, which can lead to the underestimation of P_0 by orders of magnitude (Dahley et al., 2023). For ionizable compounds, pH-dependent measurements thus must be re-evaluated.
- If P_{app} was close to the P_{ABL}, ABL effects were often simply calculated out by Avdeef. While this is in principle a valid approach, an uncertainty in the determined P_{app} has to be considered. A completely ABL-limited compound might still show a P_{app} slightly lower than the expected $P_{infinite}$, simply due to uncertainties in the measurement or the determination of the ABL size. In that case, P_0 cannot be extracted. We do not know which factor Avdeef applied to discard a

P_{app} value as limited by ABL effects, but our factor of 2 seems to be much more conservative.

- In our assumption, Avdeef used fixed P_{app} values to draw the limit for P_{ABL} or P_{para} of a specific reference to exclude P_{app} from evaluation. We use model predictions of $P_{infinite}$ and P_{para} that consider the individual diffusion coefficient of each compound, as well as concentration-shift effects in the presence of pH differences between aqueous layers.
- Typically, if a pH-dependence of a compound's P_{app} is detected, this is seen as a clear indication of a substantial contribution of transcellular transport. In our work, pH-dependence is analyzed for other possible reasons, such as concentration-shift effects or pH-dependent paracellular transport.
- We exclude some compounds for possible recovery issues, on the basis of our modeling.

Most of our extracted P_0 values did not change substantially when compared to the list of Avdeef, see Fig. 4a. All re-evaluated P_0 values that differ more than one log unit from the P_0 values extracted by Avdeef are the consequence of new experimental data. Furthermore, for the compounds excluded from evaluation (e.g. due to limitations by the ABL or paracellular transport) the P_0 limits are quite similar to the P_0 extracted by Avdeef, see Fig. 4b and c. The difference in our data sets is thus less in the values of extracted P_0, but more in the stricter exclusion of compounds where P_0 was not extractable. In the following paragraphs, we will go more into detail which measures were applied for this exclusion.

3.4. Exclusion criteria

A reliable P_0 could only be extracted for about 25 % of evaluated compounds. In this section, we will shed light on the applied exclusion criteria.

3.4.1. Limitation by ABL

For about 50 % of the analyzed data the extraction of P_0 was not possible because P_{app} could not be distinguished from the permeability expected if permeation was dominated by ABL effects, here called $P_{infinite}$. What makes the exclusion of ABL effects problematic is that

(i) Different experimental setups or even cell lines will result in different ABL sizes. For the evaluation these sizes must be known. We therefore extracted the ABL sizes of all evaluated references to the best of our knowledge, see Table S1-1. If possible, the fit was done with several ABL markers, to minimize the influence of experimental variations. Extracted total ABL sizes ranged from 100 to 4300 µm. Fig. S1-2a-c in Section S1-8 elucidates how different ABL sizes may
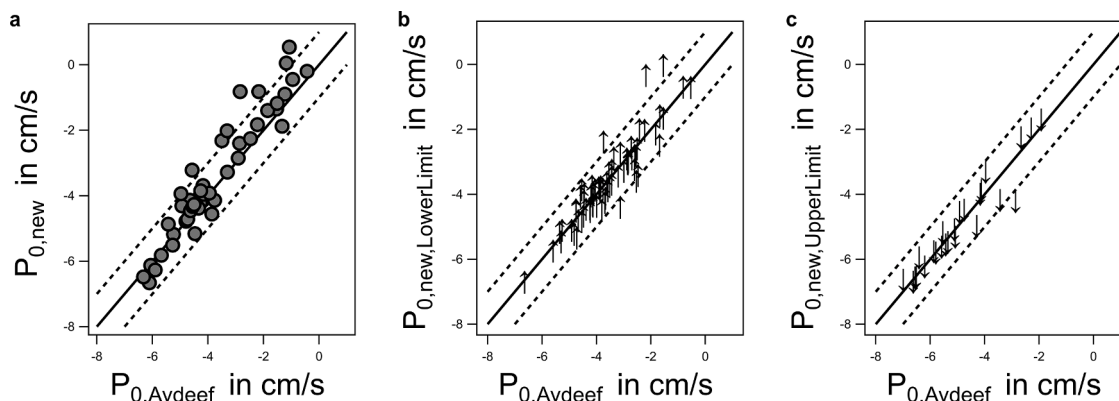

Fig. 4. Comparison of (a) extracted P_0, (b) extracted lower limits for P_0, and (c) extracted upper limits for P_0 in this work to extracted P_0 in Avdeef (2012). The solid line shows the identity line (1:1); deviations of ±1 log unit are indicated as dashed lines.

affect the P_{app} for neutral compounds, using antipyrine as an example. Our resulting ABL sizes in case of iso-pH measurements are quite similar to the ones extracted and stated by Avdeef (2012): Yazdanian et al. (1998): own 2691 µm – Avdeef 3000 µm; Irvine et al. (1999): own 568 µm – Avdeef 600 µm; Mahar Doan et al. (2002): own 1446 µm – Avdeef 1500 µm. We can thus not explain why some obviously ABL-limited compounds measured by von Richter et al. (2009) were not removed from the P_0 dataset. Even the compound with the highest experimental P_{app}, midazolam, was not excluded due to ABL-limitation.

(ii) Differences in the diffusion coefficient of molecules of different size may not be extreme, but for a molecule of MW 100 and MW 500, the predicted diffusion coefficients (Avdeef et al., 2005) differ by more than a factor of 2, which is as high as our exclusion criterium. The individual diffusion coefficients should thus not be neglected. For example in the dataset of von Richter et al. (2009), ritonavir (MW=721 g/mol) and guanabenz (MW=231 g/mol) differ by the same factor (1.2) from the respective $P_{infinite}$, our marker of ABL-limitation. However, the P_{app} values of the two ABL-limited compounds differ by a factor of 1.5, with the bigger molecule showing slower P_{app} as expected.

(iii) Concentration-shift effects may decrease the resistance of the ABL. For example in the case of weak acids if the pH in the apical compartment is lower than in the basolateral compartment, a setup that is typically used to mimic the intestine. If concentration-shift effects are not considered in the extraction the ABL size, this can lead to a considerable underestimation of the ABL size. In the case of salicylic acid (Neuhoff et al., 2005) the ABL size would have been underestimated by a factor of 3 if concentration-shift effects were not considered (Dahley et al., 2023). If such an underestimated ABL size (or the corresponding P_{app} of the acid) is applied as a threshold to detect ABL-limitation, many limitations will remain undetected, especially for bases where a negative concentration-shift (and thus an even lower P_{app}) is expected. For example, in Lee et al. (2005) a maximum log P_{app} measured for the acid isoxicam of −3.96 and a maximum of −4.4 for the neutral antipyrine and −4.45 for the base clonidine might indicate, at first glance, that only the acid was limited by ABL effects. In reality, all three are dominated by ABL effects, which is well described by our model (Eq. (3)). The difference in P_{app} can simply be explained by a positive concentration-shift effect in the basolateral ABL(+filter) for the acid due to the pH difference (6.5 to 7.4) between the apical and basolateral compartment. For the evaluation of P_{app} measured under pH differences, it is thus important to know the individual sizes of the apical and basolateral ABL. Extracted individual ABL sizes can be seen in Table S1-1. Fig. S1-2d-i elucidates how different ABL sizes may affect the P_{app} for ionizable compounds, such as the acid naproxen and the base alprenolol.

(iv) The concentration-shift is also problematic in so far that for ionizable compounds it can lead to a significant pH-dependence of P_{app}, even when P_{app} is dominated by the diffusion through the aqueous layers. ABL effects might thus mimic a typical P_{app} curve expected for P_{app} determined by transcellular transport, as is the case with verapamil (Dahley et al., 2023). The widespread assumption that a pH-dependence of P_{app} indicates a substantial contribution of P_0 is thus problematic for ionizable compounds measured at pH differences, such as ibuprofen in Lee et al. (2005) (see Section S1-9 for the modeled P_{app}), or extremely hydrophobic compounds that may even be limited by the diffusion through the cytosol, such as propranolol (Dahley et al., 2023), even in the absence of applied pH differences between both compartments. Nevertheless, if the iso-pH method is used, a change in experimental pH may still be useful to extract P_0. For example, in the case of quinidine, the measurements at pH 7.4 could not be distinguished from the ABL, but a measurement at pH 6 allowed for the extraction of P_0, see Fig. S1-3.

3.4.2. Limitations by P_{para}

For about 16 % of the analyzed data the extraction of P_0 was not possible because P_{app} could not be discerned from P_{para}. Paracellular transport will depend on the cell type, the experimental setup, and will be compound specific. Thus, while we predicted P_{para} for a typical cell assay, reference specific factors were determined (see detailed definition in Section 2.5 in methods), and are listed in Table S1-2. The determined reference specific factors ranged from 0.08 (very tight junctions) (Yamashita et al., 2000) to 1.39 (Von Richter et al., 2009). If appropriate pH-dependent measurements were available, a fit was used to determine a compound specific experimental P_{para}. For less hydrophobic compounds, P_{app} will in some setups get lost in P_{para}, while for other setups with tighter junctions, a clear P_0 might be extractable, see the example of cimetidine in Fig. S1-4 in Section S1-10.

3.4.3. Recovery issues

Recovery issues are most relevant for hydrophobic compounds that strongly sorb to matrices such as lipid or protein. Unfortunately, most references do not state compound specific recovery values, or often do not even mention recovery at all. Then, no correction *via* Eq. (2) is possible. Moreover, since most hydrophobic compounds have high membrane permeabilities (Bittermann and Goss, 2017), their permeation is in most cases limited by the diffusion through the ABL. If now the donor compartment is not in steady state with the cells/cytosol, the correction *via* Eq. (2) will fail. An extreme thought experiment: if the apical compartment was infinitely large, the recovery would be near 100 %, even when retention would reduce P_{app} substantially. In a less extreme version this can be seen for the example of felodipine (Neuhoff et al., 2007): for this experimental setup we would expect a log P_{app} of −3.97 if we assume that the ABL dominates permeation. Yet, log P_{app} values of −4.70 and −4.65 have been measured for the apical to basolateral direction and the basolateral to apical direction, respectively. With recoveries of 48 % and 70 %, the respective corrected values would be −4.38 and −4.50. These P_{app} values would be categorized as membrane limited in our system, since they differ by more than a factor of 2 from the ABL-limited P_{app}. However, measurements with added albumin clearly show that the compound is ABL-limited. We simulated the experiment with our 3-compartment model. Using predicted partition coefficients for the compounds binding to lipid and protein, we had to increase the total sorption by an artificial factor of 2 to get similar recoveries (39 % and 82 %, respectively). Our model thus reproduced the direction-dependent recovery, a phenomenon that was also reported in Heikkinen et al. (2009). A small deviation is not surprising, and might be a consequence of using typical MDCK lipid/protein content in the calculation, while Caco-2 cells were used in the experiment. It could also stem from simple variations in lipid/protein content, or errors in the prediction of the partition coefficients. As can be seen in Fig. S1-5e in Section S1-11, steady state between the donor compartment and the cytosol is not reached within the whole experimental duration for the b to a direction, which explains the higher recovery than in the a to b direction, where steady state is reached before the end of the experiment, see Fig. S1-5b. Interestingly, we found that the addition of bovine serum albumin (BSA) in the receiver compartment not only serves to maintain sink conditions (a well-known phenomenon) (Neuhoff et al., 2007), but our results indicate that compound bound to BSA also helped overcome the ABL in the receiver compartment by so-called facilitated transport (Larisch and Goss, 2018). Simply increasing the receiver volume in the model to simulate perfect sink conditions only slightly changed modeled log P_{app} (from −4.58 to −4.55 for a to b, and −4.49 to −4.31 for b to a), because the concentrations retained in the cytosol did not change substantially, see Fig. S1-6. Additionally, assuming effective facilitated transport (calculating the ABL permeability in the receiver compartment increased by a factor of 20 due to facilitated transport) restored nearly 100 % recovery and increased log P_{app} to −3.7 and −3.9, respectively. The cytosolic concentration was reduced substantially, see Fig. S1-7. These permeability values are even slightly higher than would

be expected if no BSA was added and if there was no retention in the cells, and the modeled values are quite similar to the experimental log P_{app} of -3.8 measured with BSA. This indeed indicates that the receiver ABL might be overcome by the compound bound to BSA as well as by the freely dissolved compound.

Unfortunately, in literature details necessary to simulate retention are often not stated (such as sampled volume at each timepoint, experimental recovery to validate simulation). Often we do not know the exact relation of the ABL size of the basolateral and apical compartment, there remain strong uncertainties in cell lipid/protein content, other sorption matrixes may be relevant, and the predictions of partition coefficients remain uncertain, with typical errors of about 1 log unit (Ulrich et al., 2021). For ionizable compounds, ideally the individual ABL sizes should be known to calculate the concentration-shift effects. An exact evaluation of all literature values for retention is thus not possible.

If we simulate P_{app} and the recovery for a fictive neutral compound of 350 g/mol limited by ABL permeability, and systematically vary $K_{lip/w}$, then P_{app} and recovery decrease with increasing $K_{lip/w}$, substantially so above log $K_{lip/w}$ 3, see Fig. 5a. In that range, also the P_{app} values corrected for recovery differ from the expected value, and the correction fails more strongly, the higher $K_{lip/w}$. For Fig. 5a, which was modeled with the ABL used for felodipine in the last section, this corresponds roughly to a recovery of 80 % at log $K_{lip/w}$ 3.

Furthermore, the size of the ABL influences this effect: If the total ABL size is increased, P_{app} decreases even more with $K_{lip/w}$, and the
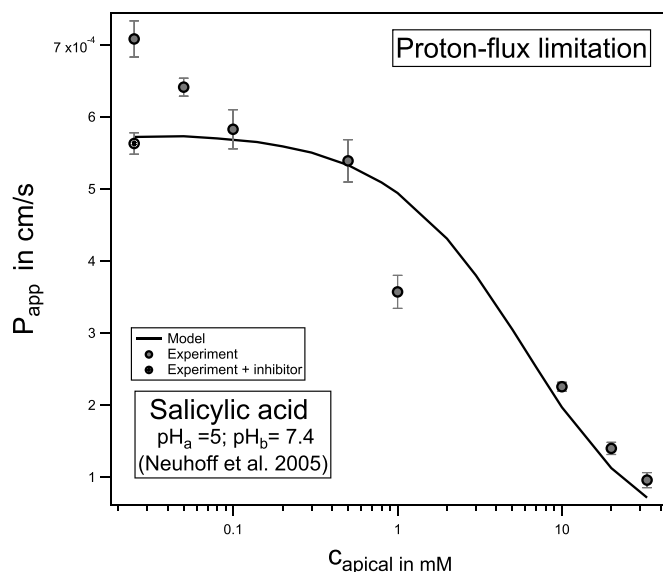

Fig. 6. Modeled P_{app} using the adapted model for proton flux limitation, plotted against the applied donor concentration in the apical compartment. Experimental data taken from Neuhoff et al., Fig. 6 (Neuhoff et al., 2005).
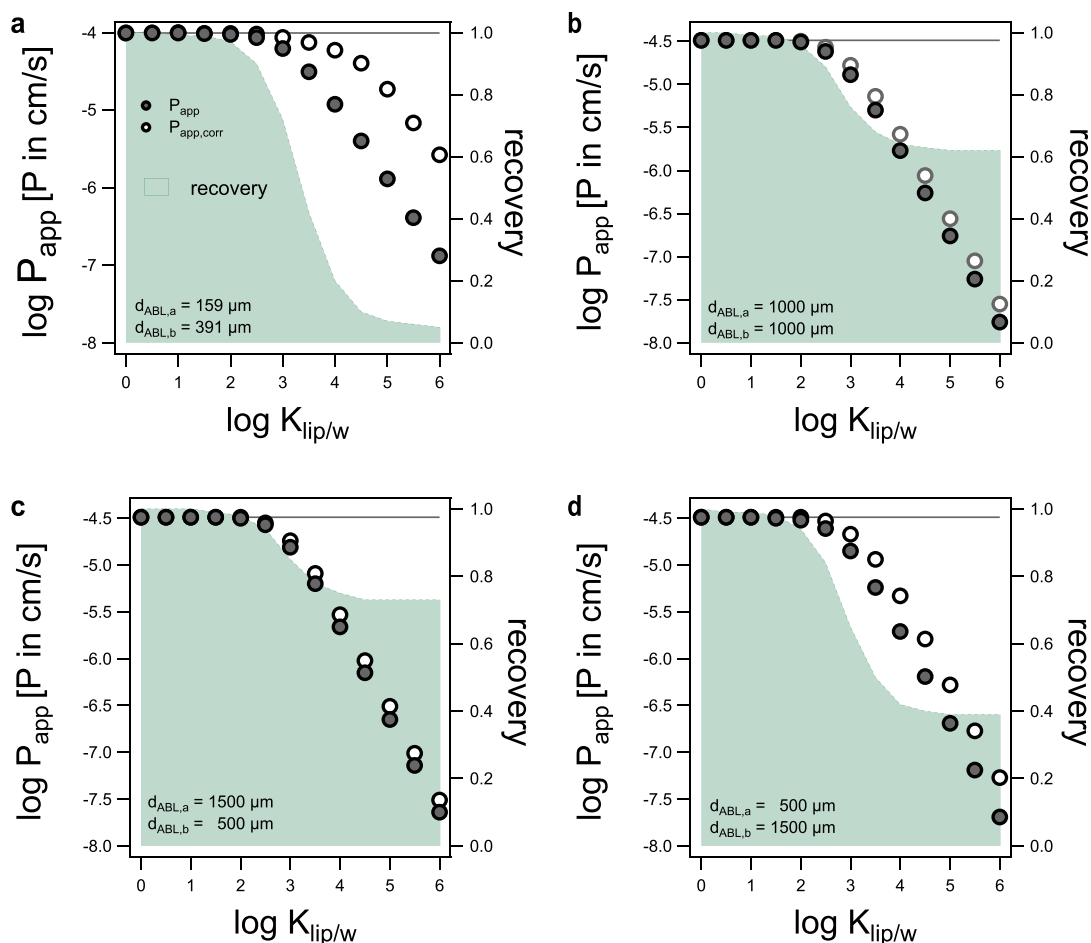

Fig. 5. Change of modeled P_{app} if $K_{lip/w}$ is varied, with varying ABL sizes: (a) ABL sizes of 159 µm and 391 µm in the apical and basolateral compartment respectively (b) 1000 µm and 1000 µm (c) 1500 µm and 500 µm, and (d), 500 µm and 1500 µm. The receiver compartment volume was increased in the simulation by a factor of 1000, to guarantee sink conditions. The horizontal line represents the P_{app} expected if there were no recovery issues.

corrected P_{app} values differ more profoundly from the expected value than for the smaller ABL (compare Fig. 5a and b). At the same time, the modeled recovery is higher. Not only the total ABL size is relevant, but its distribution between apical and basolateral compartment: The thicker the apical ABL, the higher the modeled recovery (compare Fig. 5b–d). This may seem counter-intuitive, but the higher recovery does not allow for a better corrected P_{app}. It is only a consequence of the apical compartment not being in equilibrium with the cytosol. Thus, smaller ABL do not only seem advantageous to avoid ABL-limitations, but also to avoid recovery issues.

Compounds with log $D_{lip/w} > 3$ (either predicted using COSMOmic (Bittermann et al., 2014) or LSERD (Ulrich et al., 2017), see Tables S1-5 and S2-3) that were not clearly ABL-limited according to their P_{app}, were thus assigned a special category "recovery", and assigned a greater than value, since it is extremely likely that recovery effects masked their ABL-limitation. Note that this is only a crude estimation, since $D_{lip/w}$ was simply calculated for pH 7.4, not accounting for potential pH differences and concentration-shift effects for ionizable compounds, ion-trapping effects in organelles such as lysosomes (Heikkinen et al., 2009), different experimental setups and cell lines. Yet overall, only 14 (quite hydrophobic) compounds were excluded due to the simplistic threshold. The P_{app} of seven compounds that were categorized as dominated by paracellular transport might potentially be limited by recovery issues as well, their upper limit might thus be severely underestimated.

For one reference (Summerfield et al. (2007), where extremely hydrophobic compounds were measured, we suspect strong issues with recovery, which might have been masked by the apical compartment not being in equilibrium with the cytosol. Although we were able to determine the ABL size from standard markers, ABL-limited P_{app} could not be reliably detected with our usual limit of P_{app} less than a factor 2 below $P_{infinite}$. Not considering zwitterions or paracellular dominated compounds, there were 17 overlapping compounds with measurements from other references(Aungst et al. (2000), Dahley et al. (2023), Irvine et al. (1999), Mahar Doan et al. (2002) and Von Richter et al. (2009)), that should clearly be ABL-limited in the setup of Summerfield according to the other literature values. Yet, 10 of the 17 respective P_{app} are more than a factor of 2 below the expected ABL-limited P_{app}, and would thus be classified incorrectly with our decision criterium. All P_{app} of this reference could thus only be used to extract minimal P_0, since ABL influences could not reliably be excluded (category: summerfield-recovery). Only the P_{app} values of 6 compounds could not be excluded by our conventional recovery threshold and were excluded based on their source.

3.4.4. Bidirectional transport

In case of active transport, P_{app} values measured in opposite direction (a to b and b to a) will differ. Usually, efflux ratios (ER; $P_{app}^{b \to a} / P_{app}^{a \to b}$) of at least 1.5 (Schwab et al., 2003) or 2 (Bokulic et al., 2022) have been used to identify active transport. For ionizable compounds, pH differences can also lead to significant efflux ratios, even in the absence of active transport, an effect reported already by Neuhoff et al. (2005) as passive efflux, see Section S1-12.

It has often been attempted to extract the "real" P_{app} from P_{app} dominated by active transport by taking the mean of both values. In this study, we refrain from doing so, for various reasons: The correction does not consider that (i) one or both values might be limited by ABL or paracellular transport, that (ii) there may be transport through both the apical and basolateral membrane, that (iii) there may be a surface area difference between both membranes due to microvilli, that (iv) there may be a possible influence of the cytosol, and that (v) the difference might be a consequence of sink or recovery issues.

Most problematic is the potential limitation by ABL or P_{para}: If for example P_{app} in a to b direction is limited by P_{para}, there is no way to extract P_0 from the mean, since the compound may be transported in b to a direction solely by active transport. Take the permanent ion

rhodamine 123 as an example. Although its P_0 is insubstantial, there is still a substantial flux in b to a direction (Troutman and Thakker, 2003). The P_{app} values in a to b direction for lamivudine (De Souza et al., 2009) and vincristine (Garberg et al., 2005) did not exceed P_{para}, an extraction of P_0 was thus not possible. Taking the mean would lead to an incorrect, overestimated P_0 value. In contrast, if P_{app} was ABL-limited, taking the mean would underestimate P_0.

3.4.5. Proton flux limitation

Although a potential proton flux limitation affecting the P_{app} of ABL-limited weak acids or bases has been discussed in the biophysicist community (Antonenko et al., 1997, 1993), in Caco-2/MDCK experiments it is usually just assumed that the buffer concentrations in the incubation medium are high enough to keep the pH stable, also within the ABL adjacent to the membrane. Here, we set out to assess whether this assumption is true. As a first step, we validated the adjusted model (asymmetric ABL, additional buffers, see Methods for details on the adjustments) by simulating the effect of increasing compound concentration (0.025–33 mM) on P_{app} measured for salicylic acid by Neuhoff et al. (2005) across a Caco-2 monolayer, see Fig. 7.

The model matches the experimental data well. Slight deviations in the low concentration range can be explained by active transport observed by the experimenters. There is no fit involved, the decrease in P_{app} simply results from the model, with the proton transport calculated for the buffer HBSS used in the experiment, see Table S1-4 for the used input parameters.

Although the model does not account for the cytosol, this of no consequence for salicylic acid here due to the positive concentration-shift effect within the cytosol, which further reduces the resistance of the cytosol. Although cytosolic effects may play a role in other scenarios, this would only reduce the effect of proton limitations, so the model depicts the worst-case scenario.

Fig. 7 shows the resulting pH gradients across the ABL. Up to 0.1 mM, the buffer capacity suffices to keep the pH stable. Fig. S1-8 in Section S1-13 additionally shows the resulting weak acid gradients.

We used the model to simulate typical pH gradients 7.4/7.4 and 6.5/7.4 for typical weak acids and bases (salicylic acid and amantadine), and also varied ABL sizes, pK_a and membrane permeability for generic compounds (data not shown). In no case were there any limitations as long the concentrations were kept below 100 μM, which is the case for almost all measurements from literature we analyzed.

Hayeshi et al. (2006) used concentrations up to 500 μM, but neither did the experimental P_{app} decrease with increasing concentration, nor did our model show a limiting effect due to proton flux limitation for
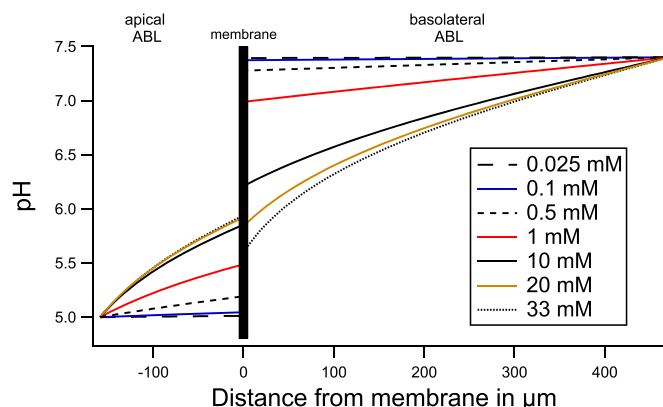

Fig. 7. Resulting pH gradients across the apical and basolateral ABL for salicylic acid at various donor (apical) compound concentrations. The black vertical line represents the membrane, negative values represent the distance from the membrane in the apical ABL, positive values the distance in the basolateral ABL. Bulk apical pH was 5, bulk basolateral pH was 7.4.

genistein or quercetin.

We conclude that for the extraction of P_0, the effect of proton flux limitation played no role in this work. Yet, it is common to saturate active transport with high compound concentrations, so one should keep in mind that such effects might occur when selecting the donor concentrations and buffer composition.

3.4.6. Sink conditions

We randomly checked the fastest compounds of different references for sink conditions. In no case did we find P_{app} changing by more than a factor of 2 when correcting for missing sink conditions, in most cases sink conditions were fulfilled. We did thus not correct for sink conditions, and no P_{app} values were excluded for that reason. But one reference (Thiel-Demby et al. (2009) used the standard correction for sink conditions as described by Tran et al. (2004) that does not consider pH differences across the cell layer, although a pH difference of pH 5.5 to pH 7.4 was applied. For ionizable compounds, the published P_{app} (Thiel-Demby et al., 2009) measured with pH difference thus have to be considered with care. Since the raw data was not published, a subsequent correction was not possible.

4. Conclusion

In this work, we looked at potential factors that might interfere with the extraction of P_0 values from P_{app} values determined in Caco-2 or MDCK assays. Limitations due to ABL and paracellular transport, as well as recovery, turned out to be the most decisive factors. Proton flux limitation in the ABL proved to be irrelevant under normal experimental conditions, but our modeling underlined the importance of a well-buffered system. Finally, only for about a quarter of the compounds analyzed in this work could P_0 values reliably be extracted. Whether or not the P_0 of a compound can be extracted depends mostly on the compound itself: For high membrane permeabilities, ABL-limitations may only be avoidable by adjusting the pH, and even then P_0 might still not be extractable, as the example of verapamil shows (Dahley et al., 2023). For low membrane permeability, P_{app} might never exceed paracellular transport. The range, however, in which membrane permeability can be extracted, can be extended by the right setup: A smaller ABL size, tighter junctions, the use of inhibitor, or the variation of external pH.

Our strict exclusion (factor 2) will ultimately also have excluded some compounds for which extraction would have been possible, but only additional experimental data can help to make a more reliable classification. However, this was necessary to create a more reliable dataset. In an upcoming publication, we will use this new list of reliable P_0 to relate P_0 from Caco-2 and MDCK experiments to P_0 predicted by the solubility diffusion model, a relationship that has so far remained unclear due to a large number of incorrectly extracted P_0 values (Dahley et al., 2022).

Funding

This research did not receive any specific grant from funding agencies in the public, commercial, or not-for-profit sectors.

CRediT authorship contribution statement

Andrea Ebert: Formal analysis, Investigation, Methodology, Writing – original draft. **Carolin Dahley:** Investigation, Writing – review & editing. **Kai-Uwe Goss:** Conceptualization, Writing – review & editing.

Declaration of competing interest

The authors declare that they have no known competing financial interests or personal relationships that could have appeared to influence the work reported in this paper.

Data availability

Data will be made available on request.

Supplementary materials

Supplementary material associated with this article can be found, in the online version, at doi:10.1016/j.ejps.2024.106699.

References

Adson, A., Burton, P.S., Raub, T.J., Barsuhn, C.L., Audus, K.L., Ho, N.F.H., 1995. Passive diffusion of weak organic electrolytes across Caco-2 cell monolayers: uncoupling the contributions of hydrodynamic, transcellular, and paracellular barriers. J. Pharm. Sci. 84, 1197–1204. https://doi.org/10.1002/jps.2600841011.

Agarwal, S., Jain, R., Pal, D., Mitra, A.K., 2007. Functional characterization of peptide transporters in MDCKII-MDR1 cell line as a model for oral absorption studies. Int. J. Pharm. 332, 147–152. https://doi.org/10.1016/j.ijpharm.2006.09.056.

Alsenz, J., Haenel, E., 2003. Development of a 7-day, 96-well Caco-2 permeability assay with high-throughput direct UV compound analysis. Pharm. Res. 20, 1961–1969. https://doi.org/10.1023/B:PHAM.0000008043.71001.43.

Antonenko, Y.N., Denisov, G.A., Pohl, P., 1993. Weak acid transport across bilayer lipid membrane in the presence of buffers. Theoretical and experimental pH profiles in the unstirred layers. Biophys. J. 64, 1701–1710. https://doi.org/10.1016/S0006-3495(93)81542-X.

Antonenko, Y.N., Pohl, P., Denisov, G.A.A., 1997. Permeation of ammonia across bilayer lipid membranes studied by ammonium ion selective microelectrodes. Biophys. J. 72, 2187–2195. https://doi.org/10.1016/S0006-3495(97)78862-3.

Artursson, P., Karlsson, J., 1991. Correlation between oral drug absorption in humans and apparent drug permeability coefficients in human intestinal epithelial (Caco-2) cells. Biochem. Biophys. Res. Commun. 175, 880–885. https://doi.org/10.1016/0006-291X(91)91647-U.

Artursson, P., Palm, K., Luthman, K., 2012. Caco-2 monolayers in experimental and theoretical predictions of drug transport. Adv. Drug Deliv. Rev. 64, 280–289. https://doi.org/10.1016/j.addr.2012.09.005.

Aungst, B.J., Nguyen, N.H., Bulgarelli, J.P., Oates-Lenz, K., 2000. The influence of donor and reservoir additives on Caco-2 permeability and secretory transport of HIV protease inhibitors and other lipophilic compounds. Pharm. Res. 17, 1175–1180. https://doi.org/10.1023/A:1026402410783.

Avdeef, A., 2012. Absorption and drug development: solubility, permeability, and charge state. ed Jurnal Penelitian Pendidikan Guru Sekolah Dasar, 2nd ed. John Wiley & Sons. Hoboken N.J.

Avdeef, A., 2010. Leakiness and size exclusion of paracellular channels in cultured epithelial cell monolayers–interlaboratory comparison. Pharm. Res. 27, 480–489. https://doi.org/10.1007/s11095-009-0036-7.

Avdeef, A., Artursson, P., Neuhoff, S., Lazorova, L., Gråsjö, J., Tavelin, S., 2005. Caco-2 permeability of weakly basic drugs predicted with the double-sink PAMPA pKaflux method. Eur. J. Pharm. Sci. 24, 333–349. https://doi.org/10.1016/j.ejps.2004.11.011.

Avdeef, A., Nielsen, P.E., Tsinman, O., 2004. PAMPA - a drug absorption *in vitro* model: 11. Matching the *in vivo* unstirred water layer thickness by individual-well stirring in microtitre plates. Eur. J. Pharm. Sci. 22, 365–374. https://doi.org/10.1016/j.ejps.2004.04.009.

Avdeef, A., Tam, K.Y., 2010. How well can the caco-2/madin-darby canine kidney models predict effective human jejunal permeability? J. Med. Chem. 53, 3566–3584. https://doi.org/10.1021/jm901846t.

Bednarczyk, D., 2021. Passive influx and ion trapping are more relevant to the cellular accumulation of highly permeable low-molecular-weight acidic drugs than is organic anion transporter 2. Drug Metab. Dispos. 49, 648–657. https://doi.org/10.1124/DMD.121.000425.

Bermejo, M., Avdeef, A., Ruiz, A., Nalda, R., Ruell, J.A., Tsinman, O., González, I., Fernández, C., Sánchez, G., Garrigues, T.M., Merino, V., 2004. PAMPA - a drug absorption *in vitro* model: 7. Comparing rat *in situ*, Caco-2, and PAMPA permeability of fluoroquinolones. Eur. J. Pharm. Sci. 21, 429–441. https://doi.org/10.1016/j.ejps.2003.10.009.

Bhardwaj, R.K., Herrera-Ruiz, D., Sinko, P.J., Gudmundsson, O.S., Knipp, G., 2005. Delineation of human peptide transporter 1 (hPepT1)-mediated uptake and transport of substrates with varying transporter affinities utilizing stably transfected hPepT1/Madin-Darby canine kidney clones and Caco-2 cells. J. Pharmacol. Exp. Ther. 314, 1093–1100. https://doi.org/10.1124/jpet.105.087148.

Bittermann, K., Goss, K.U., 2017. Predicting apparent passive permeability of Caco-2 and MDCK cell-monolayers: a mechanistic model. PLOS One 12, 1–20. https://doi.org/10.1371/journal.pone.0190319.

Bittermann, K., Spycher, S., Endo, S., Pohler, L., Huniar, U., Goss, K.U., Klamt, A., 2014. Prediction of phospholipid-water partition coefficients of ionic organic chemicals using the mechanistic model COSMOmic. J. Phys. Chem. B 118, 14833–14842. https://doi.org/10.1021/jp509348a.

Bokulic, A.N.A., Padovan, J., Stupin-Polancec, D., Milic, A., 2022. Isolation of MDCK cells with low expression of mdr1 gene and their use in membrane permeability screening. Acta Pharm. 72, 275–288. https://doi.org/10.2478/acph-2022-0003.

Braun, A., Hämmerle, S., Suda, K., Rothen-Rutishauser, B., Günthert, M., Krämer, S.D., Wunderli-Allenspach, H., 2000. Cell cultures as tools in biopharmacy. Eur. J. Pharm. Sci. 11, 51–60. https://doi.org/10.1016/S0928-0987(00)00164-0.

Butor, C., Davoust, J., 1992. Apical to basolateral surface area ratio and polarity of MDCK cells grown on different supports. Exp. Cell Res. 203, 115–127. https://doi.org/10.1016/0014-4827(92)90046-B.

Camenisch, G., Alsenz, J., Van De Waterbeemd, H., Folkers, G., 1998. Estimation of permeability by passive diffusion through Caco-2 cell monolayers using the drugs' lipophilicity and molecular weight. Eur. J. Pharm. Sci. 6, 313–319. https://doi.org/10.1016/S0928-0987(97)10019-7.

Crowe, A., 2002. The influence of P-glycoprotein on morphine transport in Caco-2 cells. Comparison with paclitaxel. Eur. J. Pharmacol. 440, 7–16. https://doi.org/10.1016/S0014-2999(02)01366-3.

Dahley, C., Garessus, E.D.G., Ebert, A., Goss, K.U., 2022. Impact of cholesterol and sphingomyelin on intrinsic membrane permeability. Biochim. Biophys. Acta - Biomembr. 1864, 183953 https://doi.org/10.1016/j.bbamem.2022.183953.

Dahley, C., Goss, K., Ebert, A., 2023. Revisiting the pK a -Flux method for determining intrinsic membrane permeability. Eur. J. Pharm. Sci. 191, 106592 https://doi.org/10.1016/j.ejps.2023.106592.

De Souza, J., Benet, L.Z., Huang, Y., Storpirtis, S., 2009. Comparison of bidirectional lamivudine and zidovudine transport using MDCK, MDCK-MDR1, and Caco-2 cell monolayers. J. Pharm. Sci. 98, 4413–4419. https://doi.org/10.1002/jps.21744.

Desmeules, J., Kanaan, M., Daali, Y., Dayer, P., 2008. Lack of interaction of the NMDA receptor antagonists dextromethorphan and dextrorphan with P-glycoprotein. Curr. Drug Metab. 9, 144–151. https://doi.org/10.2174/138920008783571765.

Ebert, A., Hannesschlaeger, C., Goss, K.U., Pohl, P., 2018. Passive permeability of planar lipid bilayers to organic anions. Biophysj 115, 1931–1941. https://doi.org/10.1016/j.bpj.2018.09.025.

Escher, B.I., Abagyan, R., Embry, M., Klüver, N., Redman, A.D., Zarfl, C., Parkerton, T.F., 2020. Recommendations for improving methods and models for aquatic hazard assessment of ionizable organic chemicals. Environ. Toxicol. Chem. 39, 269–286. https://doi.org/10.1002/etc.4602.

Furubayashi, T., Inoue, D., Nishiyama, N., Tanaka, A., Yutani, R., Kimura, S., Katsumi, H., Yamamoto, A., Sakane, T., 2020. Comparison of various cell lines and three-dimensional mucociliary tissue model systems to estimate drug permeability using an *in vitro* transport study to predict nasal drug absorption in rats. Pharmaceutics 12. https://doi.org/10.3390/pharmaceutics12010079.

Gan, L.S.L., Yanni, S., Thakker, D.R., 1998. Modulation of the tight junctions of the Caco-2 cell monolayers by H2-antagonists. Pharm. Res. https://doi.org/10.1023/A:1011944602662.

Garberg, P., Ball, M., Borg, N., Cecchelli, R., Fenart, L., Hurst, R.D., Lindmark, T., Mabondzo, A., Nilsson, J.E., Raub, T.J., Stanimirovic, D., Terasaki, T., Öberg, J.O., Österberg, T., 2005. *In vitro* models for the blood-brain barrier. Toxicol. Vitr. 19, 299–334. https://doi.org/10.1016/j.tiv.2004.06.011.

Hayeshi, R., Masimirembwa, C., Mukanganyama, S., Ungell, A.L.B., 2006. The potential inhibitory effect of antiparasitic drugs and natural products on P-glycoprotein mediated efflux. Eur. J. Pharm. Sci. 29, 70–81. https://doi.org/10.1016/j.ejps.2006.05.009.

Heikkinen, A.T., Mönkkönen, J., Korjamo, T., 2009. Kinetics of cellular retention during Caco-2 permeation experiments: role of lysosomal sequestration and impact on permeability estimates. J. Pharmacol. Exp. Ther. 328, 882–892. https://doi.org/10.1124/jpet.108.145797.

Hubatsch, I., Ragnarsson, E.G.E., Artursson, P., 2007. Determination of drug permeability and prediction of drug absorption in Caco-2 monolayers. Nat. Protoc. 2, 2111–2119. https://doi.org/10.1038/nprot.2007.303.

Irvine, J.D., Takahashi, L., Lockhart, K., Cheong, J., Tolan, J.W., Selick, H.E., Grove, J.R., 1999. MDCK (Madin-Darby canine kidney) cells: a tool for membrane permeability screening. J. Pharm. Sci. 88, 28–33. https://doi.org/10.1021/js9803205.

Karlsson, J., Artursson, P., 1991. A method for the determination of cellular permeability coefficients and aqueous boundary layer thickness in monolayers of intestinal epithelial (Caco-2) cells grown in permeable filter chambers. Int. J. Pharm. 71, 55–64. https://doi.org/10.1016/0378-5173(91)90067-X.

Karlsson, J., Ungell, A.L., Gråsjö, J., Artursson, P., 1999. Paracellular drug transport across intestinal epithelia: influence of charge and induced water flux. Eur. J. Pharm. Sci. 9, 47–56. https://doi.org/10.1016/S0928-0987(99)00041-X.

Katragadda, S., Jain, R., Kwatra, D., Hariharan, S., Mitra, A.K., 2008. Pharmacokinetics of amino acid ester prodrugs of acyclovir after oral administration: interaction with the transporters on Caco-2 cells. Int. J. Pharm. 362, 93–101. https://doi.org/10.1016/j.ijpharm.2008.06.018.

Korjamo, T., Heikkinen, A.T., Waltari, P., Mönkkönen, J., 2008. The asymmetry of the unstirred water layer in permeability experiments. Pharm. Res. 25, 1714–1722. https://doi.org/10.1007/s11095-008-9573-8.

Larisch, W., Goss, K.U., 2018. Modelling oral up-take of hydrophobic and super-hydrophobic chemicals in fish. Environ. Sci. Process. Impacts 20, 98–104. https://doi.org/10.1039/c7em00495h.

Larisch, W., Goss, K.U., 2017. Calculating the first-order kinetics of three coupled, reversible processes. SAR QSAR Environ. Res. 28, 651–659. https://doi.org/10.1080/1062936X.2017.1365763.

Lea, T., 2015. Caco-2 cell line, in: The Impact of Food Bioactives on Health. In: Vitro and Ex Vivo Models, ISBN 978-3-319-16104-4, pp. 103–111. https://doi.org/10.1007/978-3-319-16104-4_10.

Lee, J.B., Zgair, A., Taha, D.A., Zang, X., Kagan, L., Kim, T.H., Kim, M.G., Yun yeol, H., Fischer, P.M., Gershkovich, P., 2017. Quantitative analysis of lab-to-lab variability in Caco-2 permeability assays. Eur. J. Pharm. Biopharm. 114, 38–42. https://doi.org/10.1016/j.ejpb.2016.12.027.

Lee, K.J., Johnson, N., Castelo, J., Sinko, P.J., Grass, G., Holme, K., Lee, Y.H., 2005. Effect of experimental pH on the *in vitro* permeability in intact rabbit intestines and Caco-2 monolayer. Eur. J. Pharm. Sci. 25, 193–200. https://doi.org/10.1016/j.ejps.2005.02.012.

Lentz, Kimberley A., Hayashi, J., Lucisano, L.J., Polli, J.E., 2000a. Development of a more rapid, reduced serum culture system for Caco-2 monolayers and application to the biopharmaceutics classification system. Int. J. Pharm. 200, 41–51. https://doi.org/10.1016/S0378-5173(00)00334-3.

Lentz, K.A., Polli, J.W., Wring, S.A., Humphreys, J.E., Polli, J.E., 2000b. Influence of passive permeability on apparent P-glycoprotein kinetics. Pharm. Res. https://doi.org/10.1023/A:1007692622216.

Liang, E., Chessic, K., Yazdanian, M., 2000. Evaluation of an accelerated Caco-2 cell permeability model. J. Pharm. Sci. 89, 336–345. https://doi.org/10.1002/(SICI)1520-6017(200003)89:3<336::AID-JPS5>3.0.CO;2-M.

Mahar Doan, K.M., Humphreys, J.E., Webster, L.O., Wring, S.A., Shampine, L.J., Serabjit-Singh, C.J., Adkison, K.K., Polli, J.W., 2002. Passive permeability and P-glycoprotein-mediated efflux differentiate central nervous system (CNS) and non-CNS marketed drugs. J. Pharmacol. Exp. Ther. 303, 1029–1037. https://doi.org/10.1124/jpet.102.039255.

Maier-Salamon, A., Hagenauer, B., Wirth, M., Gabor, F., Szekeres, T., Jäger, W., 2006. Increased transport of resveratrol across monolayers of the human intestinal Caco-2 cells is mediated by inhibition and saturation of metabolites. Pharm. Res. 23, 2107–2115. https://doi.org/10.1007/s11095-006-9060-z.

Meng, Z., Le Marchand, S., Agnani, D., Szapacs, M., Ellens, H., Bentz, J., 2017. Microvilli morphology can affect efflux active P-glycoprotein in confluent MDCKII -hMDR1-NKI and Caco-2 cell monolayers. Drug Metab. Dispos. 45, 145–151. https://doi.org/10.1124/dmd.116.072157.

Nagahara, N., Tavelin, S., Artursson, P., 2004. Contribution of the paracellular route to the pH-dependent epithelial permeability to cationic drugs. J. Pharm. Sci. 93, 2972–2984. https://doi.org/10.1002/jps.20206.

Neuhoff, S., 2005. Role of pH and Extracellular Additives in the Caco-2 Cell Model. Uppsala University.

Neuhoff, S., Artursson, P., Ungell, A.L., 2007. Advantages and disadvantages of using bovine serum albumin and/or Cremophor EL as extracellular additives during transport studies of lipophilic compounds across Caco-2 monolayers. J. Drug Deliv. Sci. Technol. 17, 259–266. https://doi.org/10.1016/S1773-2247(07)50093-6.

Neuhoff, S., Ungell, A.L., Zamora, I, Artursson, P., 2005. pH-Dependent passive and active transport of acidic drugs across Caco-2 cell monolayers. Eur. J. Pharm. Sci. 25, 211–220. https://doi.org/10.1016/j.ejps.2005.02.009.

Neuhoff, S., Ungell, A.L., Zamora, I., Artursson, P., 2003. ph-dependent bidirectional transport of weakly basic drugs across Caco-2 monolayers: implications for drug-drug interactions. Pharm. Res. 20, 1141–1148. https://doi.org/10.1023/A:1025032511040.

Obradovic, T., Dobson, G.G., Shingaki, T., Kungu, T., Hidalgo, I.J., 2007. Assessment of the first and second generation antihistamines brain penetration and role of P-glycoprotein. Pharm. Res. 24, 318–327. https://doi.org/10.1007/s11095-006-9149-4.

Pade, V., Stavchansky, S., 1997. Estimation of the relative contribution of the transcellular and paracellular pathway to the transport of passively absorbed drugs in the Caco-2 cell culture model. Pharm. Res. https://doi.org/10.1023/A:1012111008617.

Palay, S.L., Karlin, L.J., 1959. An electron microscopic study of the intestinal villus. I. The fasting animal. J. Biophys. Biochem. Cytol. 5, 363–372. https://doi.org/10.1083/jcb.5.3.363.

Pohl, P., Saparov, S.M., Antonenko, Y.N., 1997. The effect of a transmembrane osmotic flux on the ion concentration distribution in the immediate membrane vicinity measured by microelectrodes. Biophys. J. 72, 1711–1718. https://doi.org/10.1016/S0006-3495(97)78817-9.

Polli, J.W., Wring, S.A., Humphreys, J.E., Huang, L., Morgan, J.B., Webster, L.O., Serabjit-Singh, C.S., 2001. Rational use of *in vitro* P-glycoprotein assays in drug discovery. J. Pharmacol. Exp. Ther. 299, 620–628.

Potter, T., Ermondi, G., Newbury, G., Caron, G., 2015. Relating Caco-2 permeability to molecular properties using block relevance analysis. Medchemcomm 6, 626–629. https://doi.org/10.1039/c4md00470a.

Psimadas, D., Georgoulias, P., Valotassiou, V., Loudos, G., 2012. Molecular nanomedicine towards cancer. J. Pharm. Sci. 101, 2271–2280. https://doi.org/10.1002/jps.

Raeissi, S.D., Li, J., Hidalgo, I.J., 2010. The role of an α-amino group on H+-dependent transepithelial transport of cephalosporins in Caco-2 cells. J. Pharm. Pharmacol. 51, 35–40. https://doi.org/10.1211/0022357991772060.

Robertson, S.M., Curtis, M.A., Schlech, B.A., Rusinko, A., Owen, G.R., Dembinska, O., Liao, J., Dahlin, D.C., 2005. Ocular pharmacokinetics of moxifloxacin after topical treatment of animals and humans. Surv. Ophthalmol. 50 https://doi.org/10.1016/j.survophthal.2005.07.001.

Rodríguez-Ibáñez, M., Sánchez-Castaño, G., Montalar-Montero, M., Garrigues, T.M., Bermejo, M., Merino, V., 2006. Mathematical modelling of *in situ* and *in vitro* efflux of ciprofloxacin and grepafloxacin. Int. J. Pharm. 307, 33–41. https://doi.org/10.1016/j.ijpharm.2005.09.014.

Rohatgi, A., 2022. Webplotdigitizer: version 4.6.

Ruiz-García, A., Lin, H., Plá-Delfina, J.M., Hu, M., 2002. Kinetic characterization of secretory transport of a new ciprofloxacin derivative (CNV97100) across Caco-2 cell monolayers. J. Pharm. Sci. 91, 2511–2519. https://doi.org/10.1002/jps.10244.

Schrickx, J.A., Fink-Gremmels, J., 2007. Danofloxacin-mesylate is a substrate for ATP-dependent efflux transporters. Br. J. Pharmacol. 150, 463–469. https://doi.org/10.1038/sj.bjp.0706974.

Schwab, D., Fischer, H., Tabatabaei, A., Poli, S., Huwyler, J., 2003. Comparison of *in vitro* P-glycoprotein screening assays: recommendations for their use in drug discovery. J. Med. Chem. 46, 1716–1725. https://doi.org/10.1021/jm021012t.

Schwöbel, J.A.H., Ebert, A., Bittermann, K., Huniar, U., Goss, K.U., Klamt, A., 2020. COSMO perm: mechanistic prediction of passive membrane permeability for neutral compounds and ions and its pH dependence. J. Phys. Chem. B 124, 3343–3354. https://doi.org/10.1021/acs.jpcb.9b11728.

Skolnik, S., Lin, X., Wang, J., Chen, X.H., He, T., Zhang, B., 2010. Towards prediction of *in vivo* intestinal absorption using a 96-well Caco-2 assay. J. Pharm. Sci. 99, 3246–3265. https://doi.org/10.1002/jps.22080.

Sohlenius-Sternbeck, A.K., Terelius, Y., 2022. Evaluation of ADMET predictor in early discovery drug metabolism and pharmacokinetics project work. Drug Metab. Dispos. 50, 95–104. https://doi.org/10.1124/dmd.121.000552.

Soldner, A., Benet, L.Z., Mutschler, E., Christians, U., 2000. Active transport of the angiotensin-II antagonist losartan and its main metabolite EXP 3174 across MDCK-MDR1 and Caco-2 cell monolayers. Br. J. Pharmacol. 129, 1235–1243. https://doi.org/10.1038/sj.bjp.0703150.

Summerfield, S.G., Read, K., Begley, D.J., Obradovic, T., Hidalgo, I.J., Coggon, S., Lewis, A.V., Porter, R.A., Jeffrey, P., 2007. Central nervous system drug disposition: the relationship between *in situ* brain permeability and brain free fraction. J. Pharmacol. Exp. Ther. 322, 205–213. https://doi.org/10.1124/jpet.107.121525.

Tam, K.Y., Avdeef, A., Tsinman, O., Sun, N., 2010. The permeation of amphoteric drugs through artificial membranes - An in combo absorption model based on paracellular and transmembrane permeability. J. Med. Chem. 53, 392–401. https://doi.org/10.1021/jm901421c.

Thiel-Demby, V.E., Humphreys, J.E., Williams, L.A.S.J., Ellens, H.M., Shah, N., Ayrton, A.D., Polli, J.W., 2009. Biopharmaceutics classification system: validation and learnings of an *in vitro* permeability assay. Mol. Pharm. 6, 11–18. https://doi.org/10.1021/mp800122b.

Tran, T.T., Mittal, A., Gales, T., Maleeff, B., Aldinger, T., Polli, J.W., Ayrton, A., Ellens, H., Bentz, J., 2004. Exact kinetic analysis of passive transport across a polarized confluent MDCK cell monolayer modeled as a single barrier. J. Pharm. Sci. 93, 2108–2123. https://doi.org/10.1002/jps.20105.

Troutman, M.D., Thakker, D.R., 2003. Rhodamine 123 requires carrier-mediated influx for its activity as a P-glycoprotein substrate in Caco-2 cells. Pharm. Res. 20, 1192–1199. https://doi.org/10.1023/A:1025096930604.

Ulrich, N., Endo, S., Brown, T.N., Watanabe, N., Bronner, G., Abraham, M.H., Goss, K.U., 2017. UFZ-LSER database v 3.2.1 [Internet] [WWW Document]. URL http://www.ufz.de/lserd.

Ulrich, N., Goss, K.U., Ebert, A., 2021. Exploring the octanol–water partition coefficient dataset using deep learning techniques and data augmentation. Commun. Chem. 4, 1–10. https://doi.org/10.1038/s42004-021-00528-9.

Volpe, D.A., 2004. Permeability classification of representative fluoroquinolones by a cell culture method. AAPS J. 6, 1–6. https://doi.org/10.1208/ps060213.

Von Richter, O., Glavinas, H., Krajcsi, P., Liehner, S., Siewert, B., Zech, K., 2009. A novel screening strategy to identify ABCB1 substrates and inhibitors. Naunyn. Schmiedebergs. Arch. Pharmacol. 379, 11–26. https://doi.org/10.1007/s00210-008-0345-0.

Wang, Q., Rager, J.D., Weinstein, K., Kardos, P.S., Dobson, G.L., Li, J., Hidalgo, I.J., 2005. Evaluation of the MDR-MDCK cell line as a permeability screen for the blood-brain barrier. Int. J. Pharm. 288, 349–359. https://doi.org/10.1016/j.ijpharm.2004.10.007.

Wohnsland, F., Faller, B., 2001. High-throughput permeability pH profile and high-throughput alkane/water log P with artificial membranes. J. Med. Chem. 44, 923–930. https://doi.org/10.1021/jm001020e.

Yamashita, S., Furubayashi, T., Kataoka, M., Sakane, T., Sezaki, H., Tokuda, H., 2000. Optimized conditions for prediction of intestinal drug permeability using Caco-2 cells. Eur. J. Pharm. Sci. 10, 195–204. https://doi.org/10.1016/S0928-0987(00)00076-2.

Yazdanian, M., Glynn, S.L., Wright, J.L., Hawi, A., 1998. Correlating partitioning and Caco-2 cell permeability of structurally diverse small molecular weight compounds. Pharm. Res.

Yee, S., 1997. *In vitro* permeability across Caco-2 cells (colonic) can predict *in vivo* (small intestinal) absorption in man - Fact or myth. Pharm. Res. 14, 763–766. https://doi.org/10.1023/A:1012102522787.

Young, A.M., Audus, K.L., Proudfoot, J., Yazdanian, M., 2006. Tetrazole compounds: the effect of structure and pH on Caco-2 cell permeability. J. Pharm. Sci. 95, 717–725. https://doi.org/10.1002/jps.20526.

Yu, L., Zeng, S., 2010. Transport characteristics of zolmitriptan in a human intestinal epithelial cell line Caco-2. J. Pharm. Pharmacol. 59, 655–660. https://doi.org/10.1211/jpp.59.5.0005.

Zhang, T., Applebee, Z., Zou, P., Wang, Z., Diaz, E.S., Li, Y., 2022. An *in vitro* human mammary epithelial cell permeability assay to assess drug secretion into breast milk. Int. J. Pharm. X 4, 100122. https://doi.org/10.1016/j.ijpx.2022.100122.

Zhao, R., Raub, T.J., Sawada, G.A., Kasper, S.C., Bacon, J.A., Bridges, A.S., Pollack, G.M., 2009. Breast cancer resistance protein interacts with various compounds *in vitro*, but plays a minor role in substrate efflux at the blood-brain barrier. Drug Metab. Dispos. 37, 1251–1258. https://doi.org/10.1124/dmd.108.025064.